

# Detecting Cosmic Strings in the CMB with the Canny Algorithm

Stephen Amsel<sup>1)</sup>, Joshua Berger<sup>2)</sup>, and Robert H. Brandenberger<sup>1)</sup>

<sup>1)</sup> *Department of Physics, McGill University, Montréal, QC, H3A 2T8, Canada and*

<sup>2)</sup> *Department of Physics, Cornell University, Ithaca, NY, , USA*

(Dated: November 6, 2018)

Line discontinuities in cosmic microwave background anisotropy maps are a distinctive prediction of models with cosmic strings. These signatures are visible in anisotropy maps with good angular resolution and should be identifiable using edge detection algorithms. One such algorithm is the Canny algorithm. We study the potential of this algorithm to pick out the line discontinuities generated by cosmic strings. By applying the algorithm to small-scale microwave anisotropy maps generated from theoretical models with and without cosmic strings, we find that, given an angular resolution of several minutes of arc, cosmic strings can be detected down to a limit of the mass per unit length of the string which is one order of magnitude lower than the current upper bounds.

PACS numbers: 98.80.Cq

## I. INTRODUCTION

Cosmic strings [1] are one-dimensional topological defects which arise during phase transitions in the very early universe. Since they carry energy, they will lead to density fluctuations and cosmic microwave background (CMB) anisotropies (see e.g. [2] for reviews on cosmic strings and structure formation). Causality implies that the network of strings which forms during the phase transition contains infinite strings. Once formed in the early universe, the network of strings will approach a “scaling solution” which is characterized by of the order one infinite string segment in each Hubble volume, and a distribution of cosmic string loops which are the remnants of the previous evolution. In particular, this implies that in any theory which admits cosmic strings, a network of strings will be present during the time period relevant to the CMB, namely between the time of recombination  $t_{rec}$  and the present time  $t_0$ .

A network of cosmic strings will generate a scale-invariant spectrum of cosmological perturbations [3]. As first discussed by Kaiser and Stebbins (KS) [4], the non-Gaussian nature of the density field produced by strings will lead to a distinctive signature (which we will call KS signature) in CMB anisotropy maps, namely line discontinuities. These line discontinuities are a consequence of the non-trivial nature of the metric produced by a cosmic string: space perpendicular to a cosmic string is a cone with deficit angle given by

$$\alpha = 8\pi G\mu, \quad (1)$$

where  $\mu$  is the mass per unit length of the string and  $G$  is Newton’s gravitational constant [5]. Since cosmic strings have a tension comparable to their mass per unit length, they will typically be moving with a relativistic transverse velocity  $v$ . As illustrated in Figure 1, if we are looking at the CMB in direction of the string, we will see the photons passing on different sides of the string with a Doppler shift

$$\frac{\delta T}{T} = 8\pi\gamma(v)vG\mu, \quad (2)$$

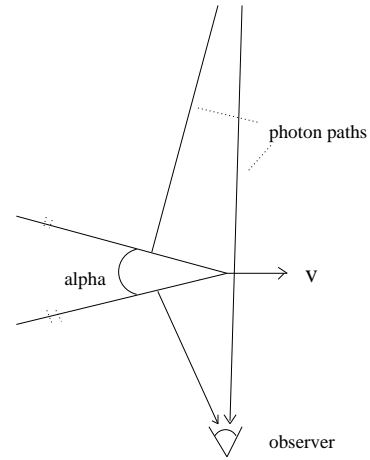


FIG. 1: Geometry of the Kaiser-Stebbins effect: Photons passing on the two sides of the moving cosmic string obtain a relative Doppler shift for the observer who is at rest.

where  $\gamma(v)$  is the relativistic gamma factor. Looking in direction of the string, we will see a line in the sky across which the CMB temperature jumps by the above amount.

Any cosmic string which photons reaching us today pass on their way from the last scattering surface will produce an effect. The most numerous strings, however, are those present close to the time of last scattering  $t_{rec}$ . At that time, the typical curvature radius of a long string segment is of the order of the Hubble radius at  $t_{rec}$ . The corresponding angular scale today is about  $1^\circ$ . In order to be able to identify the cosmic signature as a line discontinuity, as good an angular resolution as possible is required. If probed with an angular resolution not significantly smaller than  $1^\circ$ , the KS signature will be washed out. In this work we will study the potential of surveys with an angular of several minutes of arc to detect the KS signature for strings. Less important than the angular resolution of the survey is the total sky coverage, as long as it includes a sufficiently large number of Hubble patches at  $t_{rec}$ . Obviously, increasing the sky coverage will reduce the standard deviation of the results and thus

lead to some better discriminating power.

There has been surprisingly little work devoted to detecting the KS signature. An early study [6] showed that the angular resolution of the WMAP satellite would not be adequate to pick out the KS signature, even for values of  $G\mu$  for which the cosmic strings would dominate the power spectrum of density fluctuations. In order to detect the KS signature, new statistical methods must be employed. In [7], a matched filtering method was applied to the WMAP data to search for cosmic string signatures. In [8], new statistics (such as a statistic measuring the connectedness of neighboring temperature steps or a decomposition of the temperature map into constant background temperature, Gaussian noise plus straight string step discontinuities) were introduced and applied to the WMAP data to search for strings. Based on the null results of both studies, an upper bound on  $G\mu$  of  $G\mu < 10^{-6}$  could be set. However, this bound is not competitive with other existing bounds on the string tension coming from the observed acoustic peak structure of the CMB angular power spectrum [9] (which yields  $G\mu < 10^{-7}$ ) and from pulsar timing measurements [10] (which yield limits of between  $G\mu < 2 \times 10^{-8}$  and  $G\mu < 10^{-5.5}$ , the difference being due to conflicting ways [11] in which the pulsar timing data is analyzed to obtain limits on the amplitude of the stochastic background of gravitational waves, and due to different assumptions about the distribution of cosmic string loops, the main source of gravitational radiation from a string network - see [12] for a recent discussion). Note that an advantage of using the KS signature over pulsar bounds is that the KS signature is more robust (less dependent on the unknown distribution of cosmic string loops) than the pulsar bounds (which depend sensitively on the details of the cosmic string loop distribution) [32]

As discussed above, we expect to be able to set much stronger limits on  $G\mu$  from searches for the KS signature by looking at small-scale anisotropy maps, provided we find a good statistic to identify line discontinuities. The goal of this paper is to explore the potential of one specific edge detection technique, the Canny algorithm [13] to pick out these line discontinuities in CMB anisotropy maps.

One reason for the relative lack of previous work on detecting the KS signature of cosmic strings is the fact that interest in cosmic strings as a source for structure in the universe [33] decreased dramatically after the discovery of the sharpness of the acoustic peaks in the CMB angular power spectrum [14, 15]. Since perturbations seeded by strings are not coherent [16], a scenario with only cosmic strings as the source of density perturbations would only produce one broad Doppler peak rather than the observed narrow acoustic oscillations [17, 18, 19].

However, recent years have seen a resurgence of interest in cosmic strings. This was fueled by two developments. Firstly, it was realized [20] that in many supersymmetric particle physics models, cosmic strings are formed after inflation, and thus contribute to but do not completely

replace inflationary perturbations as the seeds for structure formation. Secondly, it has recently been realized that models with cosmic superstrings [21] may well be viable [22]. They could, for example, be generated as the remnant of brane annihilation processes in brane inflation models [23], or they may play an important role in inflationary models in warped backgrounds [24]. Cosmic superstrings may also be left behind after the initial Hagedorn phase in string gas cosmology [25], where they would add an additional component to the spectrum of fluctuations produced by thermal string gas fluctuations [26]. Thus, it is of great interest to find new ways to search for signatures of strings in cosmological data.

The outline of this paper is as follows: In the following section we review the Canny algorithm and describe its application to our problem. Section 3 discusses how the temperature maps with and without strings are produced, introduces the parameters chosen in the specific simulations, and presents our results. We conclude with a summary and a discussion of the caveats of the current analysis and prospects for future work.

## II. THE CANNY ALGORITHM

The Canny algorithm was developed in 1986 as a technique to detect edges in images [13] such as the two-dimensional images considered here. When applied to a map of raw data, the algorithm is intended to produce a map tracing the edges in the map, the lines across which the intensity contrast is largest.

The first step in the algorithm is to filter the data to eliminate point source noise. The filtering is achieved using a convolution of the map with a Gaussian filter. The filtering length is a free parameter in the algorithm. It must be chosen sufficiently large to eliminate unwanted point source noise, but must be smaller than the characteristic size of the structure in the maps which one is trying to identify. Let us denote the original map by  $M(i, j)$ , and the filter by  $F(i, j)$ . The filtered map  $FM$  is then given by

$$FM(i, j) = \sum_{k, l} M(i - k, j - l)F(k, l), \quad (3)$$

where the pixel points of the map are denoted by the labels  $(i, j)$ . In our simulations, the filtering length is taken to be 1.5 grid units.

The second step of the algorithm is to find the gradient of the filtered image, a vector obtained by taking the discrete derivative of the map in each of the two directions. The gradient vector at a grid point  $(i, j)$  is denoted by  $(G_x, G_y)$ , where  $G_x$  and  $G_y$  are the derivatives in the respective directions. The *edge strength*  $|G|$  at any given grid point is defined by

$$|G| = \sqrt{|G_x|^2 + |G_y|^2}, \quad (4)$$

and the *edge direction* is given by the angle

$$\theta = \arctan(G_y/G_x). \quad (5)$$

Since we are working on a grid, it makes sense to replace the edge direction by one of the eight distinguished directions on a quadratic grid, namely the four directions along the coordinate axes and the four diagonal directions.

The average maximal gradient in maps without cosmic strings (the average taken over all of our runs) is denoted by  $G_m$ . For a specific run, the maximal gradient is obtained by scanning the entire map and searching for the maximal value of the grid strength. The value of  $G_m$  is used to set the thresholds discussed below.

The next step of the Canny algorithm is to find grid points with gradients which are maximal when we vary the point in direction of the gradient. Grid points which are not local maxima of the gradient are assigned a number 0.

At this stage, two thresholds must be set, an upper and a lower threshold  $t_u$  and  $t_l$ . The algorithm first finds local maxima in the gradient along one of the four directional axes on the grid. Next, it goes through each of the list of local maxima and determines whether the gradient is greater than the upper threshold fraction of  $G_m$ , i.e.

$$|G| > t_u G_m. \quad (6)$$

Grid point thus selected are marked with a number 1. If the gradient is larger than the lower threshold fraction of  $G_m$ ,

$$|G| > t_l G_m, \quad (7)$$

the grid point is assigned a value of 1/2. For points marked with 1 or 1/2, the direction of the gradient is also stored. For each grid point with a value of 1/2, the algorithm next checks whether there is a grid point with value of 1 or 1/2 which is in a direction perpendicular to the gradient and whose gradient is parallel or next to parallel (thus three possible directions in total) to the initial gradient. If such a grid point is found, the algorithm continues until it either does not find another point satisfying the criteria or else finds a point satisfying the criteria marked with a 1. If it finds such a point, then all of the points (initially marked 1/2) found along the way are marked as 1. Neighboring (in all eight directions) grid points marked by 1 are then said to belong to the same edge. These are edges across which the gradient of the map is large.

The reason for using two thresholds is as follows: we want the algorithm to find lines with a large gradient. At the same time, we do not want noise to lead to points along a line of large gradients to be missed (and thus the lines cut) just because noise has reduced the amplitude of the edge strength at one point along the line.

In this way, the algorithm produces a list of grid points belonging to edges, and this list can be read out as a

map of edges. In our simulations, the upper and lower thresholds are  $t_u = 0.5$  and  $t_l = 0.4$ .

It is important to quantify the edge maps. A simple way to do this is to produce a histogram of edge lengths. Thus, the implementation of the Canny algorithm is arranged such as to output a list of edge lengths which can then be used to produce a histogram of edge lengths. The histogram contains useful information about the presence of edges in the map.

### III. APPLYING THE CANNY ALGORITHM TO CMB ANISOTROPY MAPS

Eventually, we would like to apply the Canny algorithm to actual CMB maps. For this initial feasibility study, however, we will apply the algorithm to theoretical maps produced in numerical simulations. We wish to compare temperature maps for the “standard” Gaussian  $\Lambda$ CDM model with maps in which a network of strings contributes a fraction  $f$  of the total power. The maps are characterized by the angular scale of the survey (we take the survey area to be square) and by the angular scale of the grid, i.e. the angular resolution of the survey.

The Gaussian maps are produced in the following way: We start with the angular power spectrum  $C_l$  of cosmic microwave anisotropies taken from the CMBFAST simulation [27] with the appropriate cosmological parameters [34]. Since we have in mind applications of our algorithm to small angular scale surveys, we perform a “flat sky” approximation [28]. We introduce a two-dimensional Cartesian coordinate system covering the survey area which we take to be rectangular, choosing the upper right corner of the survey area to be the origin of the coordinates. We need to compute the temperature field  $T_G(x, y)$  of the map at the coordinate values  $(x, y)$  corresponding to the grid points. This map is determined by an inverse fast Fourier transform from the temperature values  $\tilde{T}(\vec{k})$  in Fourier space.

For each vector  $\vec{k}$  in Fourier space, we find the integers  $l_1(k)$  and  $l_2(k)$  which bracket the  $l$  value  $l(k)$  corresponding to  $\vec{k}$  and take a linear interpolation of the values of  $C_l$ . Let us denote the result of this linear interpolation by  $C_{l(k)}$ , where  $k \equiv |\vec{k}|$ . The value of  $\tilde{T}(\vec{k})$  is then given as follows:

$$\tilde{T}(\vec{k}) = g(\vec{k}) \sqrt{C_{l(k)}}, \quad (8)$$

where  $g$  is a random variable drawn from a probability distribution with variance 1.

In the above analysis, we are singling out one grid point to be special, namely the origin. This introduces unwanted phase correlations which we overcome by superimposing the results from four separate simulations, indicated by  $T_i, i = 1, \dots, 4$ :

$$T_G(x, y) = \frac{1}{2} (T_1(x, y) + T_2(x_m - x, y_m - y) + T_3(x_m - x, y) + T_4(x, y_m - y)), \quad (9)$$

where  $x_m$  and  $y_m$  are the maximal  $x$  and  $y$  values of the survey volume (the pre-factor of 1/2 is required in order to maintain the original standard deviation).

A network of cosmic strings will produce a temperature map  $T_{CS}(x, y)$ . In the following, we take a toy model for a temperature map produced by strings introduced by Perivolaropoulos [6, 29]. The toy model takes into account that at all times between  $t_{rec}$  (the time of recombination) and the present time  $t_0$ , the network of strings is described by a scaling solution in which there are a fixed number of long string segments (strings which are not loops with radius smaller than the Hubble radius) crossing each Hubble volume. Each such string gives rise to a Kaiser-Stebbins line discontinuity (2) in the temperature map. The cosmic string network is continuously evolving via motion of the strings and string interactions which lead to the production of string loops. Thus, in each Hubble time step the string network can be taken to be uncorrelated.

In the algorithm, we divide the time interval  $t_{rec} < t < t_0$  into 15 Hubble time steps. In each time step  $t$  we lay down a network of strings at random, uncorrelated with the network at the previous time step. We take the network to consist of straight string segments of length  $\alpha_1 t$ . In order to avoid missing strings at the edges of the survey area, the survey area is extended in each direction by a Hubble distance. The program runs through all points of the simulation volume and picks points to be midpoints of a string segment with a probability chosen such that the average number of strings in the Hubble volume equals the number  $N$  of the scaling solution. The directions of the strings are chosen at random, as are the string transverse velocities. To take into account also the projection onto the last scattering surface, we add a temperature

$$\frac{\delta T}{T} = \frac{1}{2} \tilde{v} r 8\pi G\mu, \quad (10)$$

to one side of the string projection onto the last scattering surface, and subtract it from the other (so as to maintain the average temperature of the CMB). Here,  $\tilde{v}$  stands for the maximal value of  $v\gamma(v)$ , where  $v$  is the transverse velocity of the string, and  $\gamma(v)$  is the relativistic  $\gamma$  factor associated with  $v$ . Also,  $r$  is a random number between 0 and 1, to take into account both the distribution of velocities, and also projection effects (the formula (2) for the line discontinuity in temperature is modulated by an angular factor if the string velocity is not perpendicular to our line of sight to the string). The regions affected by the temperature fluctuation are rectangles on either side of the string. The depth of these rectangles in direction transverse to the direction of the string is taken to be a fraction  $f$  of the Hubble radius. The length of the string segments is taken to be  $\alpha_1$  times the Hubble radius. The survey area is always taken to correspond to the central region of the simulation area.

The free parameters of the string simulation are  $G\mu$ , the number of strings  $N$  per Hubble volume, the length

coefficients  $\alpha_1$  and  $f$ , as well as  $\tilde{v}$ . In our work, we will fix  $N = 10$ ,  $\alpha_1 = 2$ ,  $f = 1$  and  $\tilde{v} = 0.15$ . These values are representative of the results of numerical simulations of cosmic string evolution (see [2] for reviews). However, it should be kept in mind that the results for these parameters obtained using different numerical codes differ significantly.

Let us make a couple of comments on the expected dependence of the results on the value of  $N$ . As  $N$  initially increases from zero, the signature of the strings should increase since there are more strings. However, once  $N$  rises above a certain critical value, then further increasing the number  $N$  will render the string distribution more Gaussian by the Central Limit Theorem and will hence decrease the sensitivity of the Canny algorithm. We expect that the critical value of  $N$  will be the one for which the regions of the sky effected by individual string segments begin to overlap. If the strings have length comparable to the Hubble radius, the the critical value of  $N$  is expected to be less than  $N = 10$ .

Increasing the string velocity  $\tilde{v}$  will boost the line discontinuities in the temperature maps and will make our algorithm more effective. Since the weight in our statistical analysis of the edge maps comes from fairly short segments, our results are not very sensitive to the specific values of  $f$  and  $\alpha_1$ .

We are interested in using the Canny algorithm to find signatures for cosmic strings in maps which contain both Gaussian fluctuations from inflation and a cosmic string component (which is sub-dominant in terms of its contribution to the power spectrum). The total map  $T_T(x, y)$  is given by the superposition of a pure Gaussian noise map and the map produced by a distribution of strings:

$$T_T(x, y) = T_G(x, y) + T_{CS}(x, y), \quad (11)$$

and where the amplitude of the Gaussian term is adjusted such that the total angular power spectrum agrees with the COBE results [30].

The output of the Canny algorithm is a map of edges which have been picked out. In the presence of cosmic strings, we would expect more longer edges than in the absence of strings. In order to test for this effect, we produced histograms of the distribution of edge lengths for each simulation. Since both the Gaussian maps and the maps with cosmic strings are produced by a Gaussian random process (the phases of the Fourier modes for the Gaussian maps are picked at random, and for the string maps the locations of the string centers, their directions and their transverse velocity vectors are all random), we ran many ( $\tilde{N} = 50$ ) simulations for both the Gaussian map and the maps with strings. This gave us statistical error bars on the histograms of edge lengths. In turn, this allows us to assign statistical weight to the difference in the histograms. Our results are based on this analysis.

In our simulations, we consider the ‘‘Gaussian noise’’ maps to be given by a standard  $\Lambda$ CDM model with adiabatic fluctuations with a spectral index of  $n_s = 0.99$ , and with parameters  $\Omega_B = 0.046$  (baryon fraction),

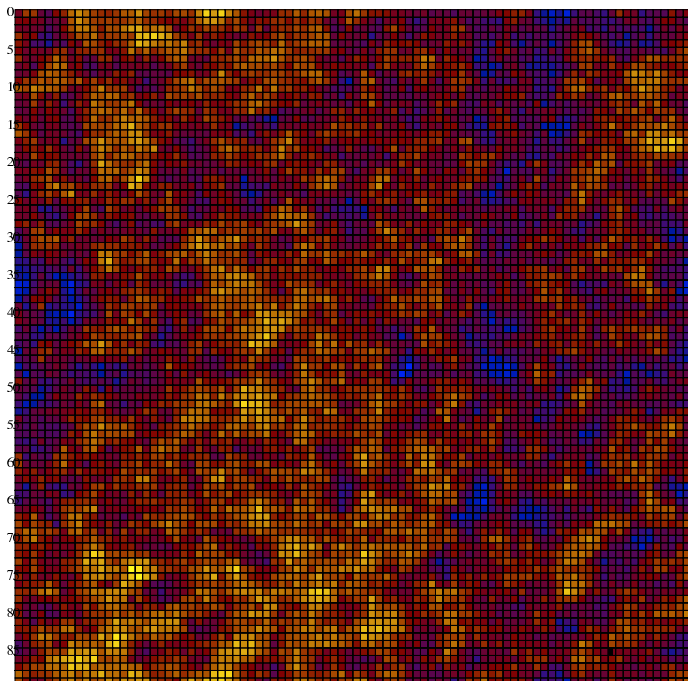


FIG. 2: Map of the CMB temperature in a  $15^2$  square of the sky for a  $\Lambda$ CDM simulation with the parameters described in the text.

$\Omega_{CDM} = 0.224$  (cold dark matter fraction),  $\Omega_{\Lambda} = 0.730$  (cosmological constant contribution), and  $H_0 = 72$  (Hubble expansion rate). No massless neutrinos, standard recombination history and a Helium fraction of  $Y = 0.24$  were assumed (in the  $C_l$  spectra which were used to construct the maps).

The parameters of the string simulation are indicated above. Our maps have angular extent 15 degrees by 15 degrees.

We fix the angular resolution and search for the minimal value of the cosmic string mass parameter  $G\mu$  for which the maps with the strings can be distinguished from the pure Gaussian maps at a statistically significant level. We demand significance at the  $3\sigma$  level.

Figure 2 shows a CMB temperature fluctuation map of a simulation without strings, and Figure 3 is the corresponding map of a simulation which includes strings according to the prescription described above.

The output of the Canny algorithm applied to the above maps is shown in Figures 4 and 5, respectively.

Based on these results, our algorithm evaluates the distribution of edge lengths and checks whether the distributions of the histograms with and without strings are statistically different. Maps with cosmic strings showed, as expected, a slight excess of edges of all lengths. This excess is more pronounced for edge lengths which lie in the non-Gaussian tail.

The results for an angular resolution of  $8'$  are presented in Table 1. In this table, the rows indicate the length  $L$  of the edge. The entries in the columns are the mean num-

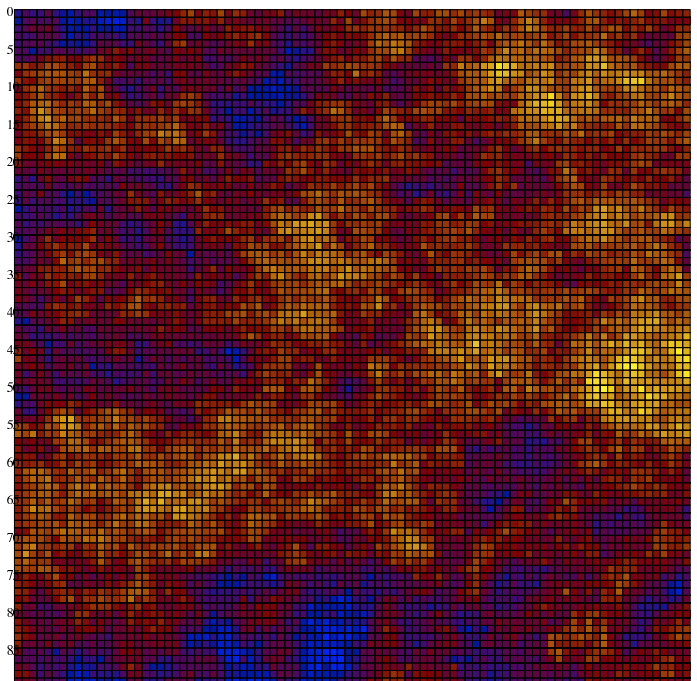


FIG. 3: Corresponding map of the CMB temperature in a simulation which includes cosmic strings with a mass per unit length parameter given by  $G\mu = 10^{-7}$  (and other parameters as described in the text).

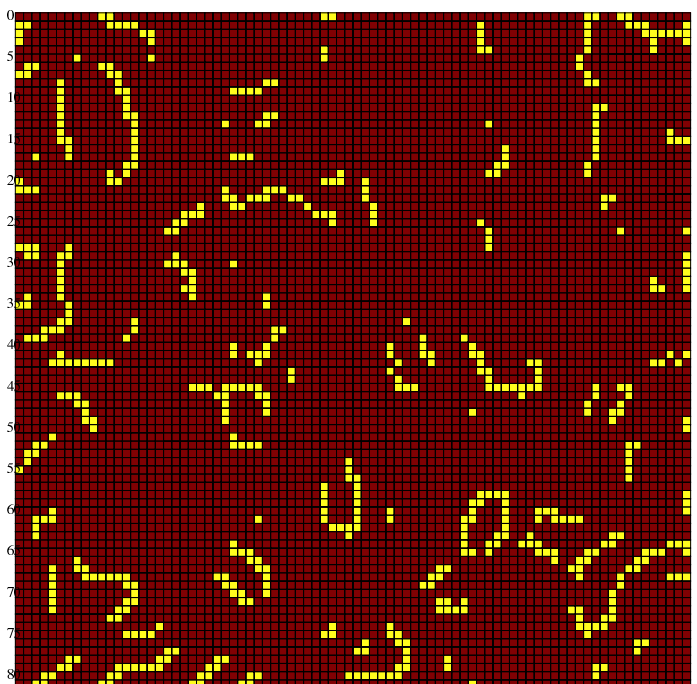


FIG. 4: Output map of the Canny algorithm showing the edges in the  $\Lambda$ CDM map of Figure 2.

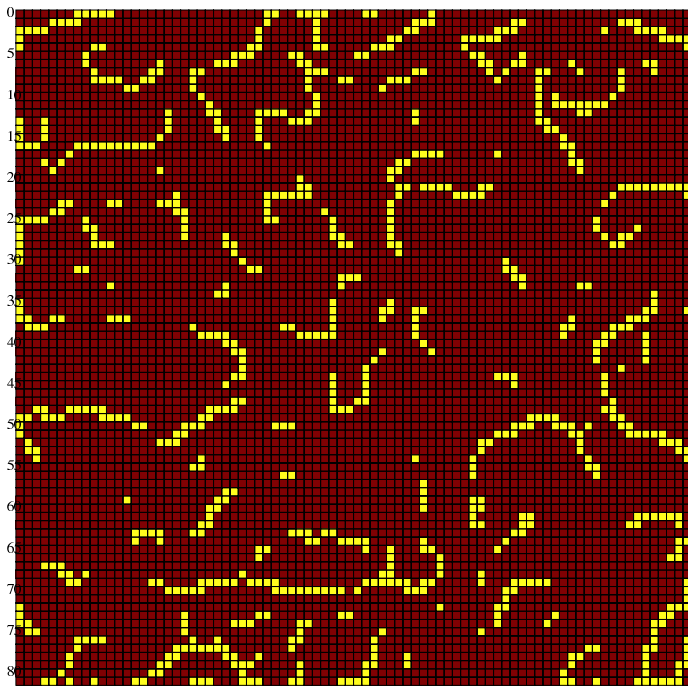


FIG. 5: Corresponding edge distribution in the map of Figure 3.

ber [standard deviation of the mean] of edges of the maps which have the respective length. The first column of numbers is for simulations without strings, the next two are for simulations including a network of strings with the indicated mass per unit length parameter. Each histogram was produced from 50 runs. From the histogram it follows that the difference between the distributions is significant (at the  $3\sigma$  level) if  $G\mu = 3.5 \times 10^{-8}$ , but not if  $G\mu = 3 \times 10^{-8}$ .

For a given angular resolution, we varied the string mass parameter  $G\mu$  to find the limiting value below which the differences in the histograms ceased to be statistically significant (using Fisher's combined probability test). Our results are summarized in Table 2.

Based on the above results, prospects for being able to use the Canny algorithm to significantly improve the limits on the cosmic string mass parameter  $G\mu$  (or detect cosmic strings) are excellent. The angular resolution of the Planck satellite experiment will be about  $5'$ , the South Pole Telescope is aiming for a resolution of  $1'$  with a field of view of 4,000 square degrees, and the resolution of the ACT telescope in Chile will be  $1.5'$ .

#### IV. CONCLUSIONS

We have suggested a new way of looking for the specific signature of cosmic strings, namely the Kaiser-Stebbins line discontinuities, in small-scale cosmic microwave anisotropy maps. Our method makes use of the Canny algorithm, an edge-detection technique used often

TABLE I: Histograms of the distribution of edge lengths  $L$ .

	no strings	$G\mu = 3 \times 10^{-8}$	$G\mu = 3.5 \times 10^{-8}$
L = 2	165.0 [2.84]	169.9 [3.60]	178.0 [3.84]
L = 3	40.0 [0.86]	42.3 [1.19]	43.6 [1.18]
L = 4	11.8 [0.51]	13.4 [0.58]	14.0 [0.57]
L = 5	4.5 [0.31]	4.8 [0.32]	5.5 [0.34]
L = 6	1.7 [0.23]	2.1 [0.21]	2.2 [0.21]
L = 7	0.66 [0.13]	0.74 [0.11]	0.84 [0.12]
L = 8	0.18 [0.07]	0.38 [0.09]	0.28 [0.07]
L = 9	0.12 [0.06]	0.1 [0.04]	0.08 [0.05]
L = 10	0.04 [0.03]	0.08 [0.04]	0.04 [0.03]

TABLE II: Critical values of the string mass parameter  $G\mu$ .

angular resolution	$G\mu$
$10'$	$4.3 \times 10^{-8}$
$9'$	$4.0 \times 10^{-8}$
$8'$	$3.1 \times 10^{-8}$

in pattern recognition.

Since the cosmic microwave temperature anisotropy maps induced by a network of cosmic strings are dominated by the strings present at the time of last scattering (when the Hubble radius, which is comparable to the correlation length of the string network at that time, is of the order of one degree), good small-scale angular resolution is essential in order to be able to detect strings. An angular resolution substantially less than  $1^\circ$  is required, otherwise the signals from the line discontinuities are washed out.

We have constructed CMB anisotropy maps which correspond to having both Gaussian "noise" with a nearly scale-invariant power spectrum from inflation and anisotropies produced by a distribution of straight string segments. Based on our numerical simulations, we find that for an angular resolution of CMB maps of  $8'$  the Canny algorithm has the potential to detect strings with a mass per unit length  $\mu$  above a value of  $G\mu \simeq 4 \times 10^{-8}$ , close to an order of magnitude better than current limits based on the CMB.

A drawback of our work is that it is based on toy model cosmic string CMB maps which are obtained by superimposing idealized line discontinuities of straight string segments, not from actual string networks. Actual string networks contain both infinite strings and string loops. The infinite strings are not completely straight, but have a curvature radius comparable to the Hubble radius. An improved analysis should start from a numerical simulation of the distribution of cosmic strings, calculate the induced temperature anisotropies taking into account of all effects following the formalism set out in [19], and then apply the Canny algorithm to the resulting maps. After completion of this work, a paper appeared [31] in

which CMB temperature maps on scales similar to the ones we are considering were constructed based on full cosmic string simulations. This work confirmed that the Kaiser-Stebbins from long string segments is the dominating visible effect, and suggested, in agreement with the message of our work, that strings should be visible in high resolution small-scale CMB anisotropy maps. However, no string-specific statistical analyses of the maps like the one we are proposing were performed in [31].

Another important issue which remains to be analyzed is the effect of instrumental noise. We have done preliminary work on this topic and modelled instrumental noise by a component to the  $C_l$  spectrum which rises rapidly as a function of  $l$  at the scale of the angular resolution of

the survey [35], becoming dominant at the angular resolution scale. Initial results show that the efficiency of the Canny algorithm is not reduced. We plan to study this question in more detail.

### Acknowledgments

This work is supported in part by a NSERC Discovery Grant, by funds from the CRC Program, and by a FQRNT Team Grant. We wish to thank Matt Dobbs, Christophe Ringeval, and in particular Gil Holder for useful discussions.

- 
- [1] T. W. B. Kibble, "Topology Of Cosmic Domains And Strings," J. Phys. A **9**, 1387 (1976);  
 Y. B. Zeldovich, "Cosmological fluctuations produced near a singularity," Mon. Not. Roy. Astron. Soc. **192**, 663 (1980);  
 A. Vilenkin, "Cosmological Density Fluctuations Produced By Vacuum Strings," Phys. Rev. Lett. **46**, 1169 (1981) [Erratum-ibid. **46**, 1496 (1981)].
- [2] A. Vilenkin and E.P.S. Shellard; *Cosmic Strings and Other Topological Defects*, (Cambridge Univ. Press, Cambridge, 1994);  
 M. B. Hindmarsh and T. W. Kibble, "Cosmic strings," Rept. Prog. Phys. **58**, 477 (1995) [arXiv:hep-ph/9411342];  
 R. H. Brandenberger, "Topological defects and structure formation," Int. J. Mod. Phys. A **9**, 2117 (1994) [arXiv:astro-ph/9310041].
- [3] N. Turok and R. H. Brandenberger, "Cosmic Strings And The Formation Of Galaxies And Clusters Of Galaxies," Phys. Rev. D **33**, 2175 (1986);  
 H. Sato, "Galaxy Formation by Cosmic Strings," Prog. Theor. Phys. **75**, 1342 (1986);  
 A. Stebbins, "Cosmic Strings and Cold Matter", Ap. J. (Lett.) **303**, L21 (1986).
- [4] N. Kaiser and A. Stebbins, "Microwave Anisotropy Due To Cosmic Strings," Nature **310**, 391 (1984).
- [5] A. Vilenkin, "Gravitational Field Of Vacuum Domain Walls And Strings," Phys. Rev. D **23**, 852 (1981).
- [6] R. Moessner, L. Perivolaropoulos and R. H. Brandenberger, "A Cosmic string specific signature on the cosmic microwave background," Astrophys. J. **425**, 365 (1994) [arXiv:astro-ph/9310001].
- [7] A. S. Lo and E. L. Wright, "Signatures of cosmic strings in the cosmic microwave background," arXiv:astro-ph/0503120.
- [8] E. Jeong and G. F. Smoot, "Search for cosmic strings in CMB anisotropies," Astrophys. J. **624**, 21 (2005) [arXiv:astro-ph/0406432];  
 E. Jeong and G. F. Smoot, "The Validity of the Cosmic String Pattern Search with the Cosmic Microwave Background," arXiv:astro-ph/0612706.
- [9] L. Pogosian, S. H. H. Tye, I. Wasserman and M. Wyman, "Observational constraints on cosmic string production during brane inflation," Phys. Rev. D **68**, 023506 (2003) [Erratum-ibid. D **73**, 089904 (2006)] [arXiv:hep-th/0304188];  
 M. Wyman, L. Pogosian and I. Wasserman, "Bounds on cosmic strings from WMAP and SDSS," Phys. Rev. D **72**, 023513 (2005) [Erratum-ibid. D **73**, 089905 (2006)] [arXiv:astro-ph/0503364];  
 A. A. Fraisse, "Limits on Defects Formation and Hybrid Inflationary Models with Three-Year WMAP Observations," JCAP **0703**, 008 (2007) [arXiv:astro-ph/0603589];  
 U. Seljak, A. Slosar and P. McDonald, "Cosmological parameters from combining the Lyman-alpha forest with CMB, galaxy clustering and SN constraints," JCAP **0610**, 014 (2006) [arXiv:astro-ph/0604335];  
 N. Bevis, M. Hindmarsh, M. Kunz and J. Urrestilla, "CMB power spectrum contribution from cosmic strings using field-evolution simulations of the Abelian Higgs model," Phys. Rev. D **75**, 065015 (2007) [arXiv:astro-ph/0605018];  
 N. Bevis, M. Hindmarsh, M. Kunz and J. Urrestilla, "Fitting CMB data with cosmic strings and inflation," arXiv:astro-ph/0702223.
- [10] F. R. Bouchet and D. P. Bennett, "Does The Millisecond Pulsar Constrain Cosmic Strings?," Phys. Rev. D **41**, 720 (1990).
- [11] V. M. Kaspi, J. H. Taylor and M. F. Ryba, "High - precision timing of millisecond pulsars. 3: Long - term monitoring of PSRs B1855+09 and B1937+21," Astrophys. J. **428**, 713 (1994);  
 S. E. Thorsett and R. J. Dewey, "Pulsar timing limits on very low frequency stochastic gravitational radiation," Phys. Rev. D **53**, 3468 (1996);  
 M. P. McHugh, G. Zalamansky, F. Vernotte and E. Lantz, "Pulsar Timing And The Upper Limits On A Gravitational Wave Background: A Bayesian Approach," Phys. Rev. D **54**, 5993 (1996);  
 A. N. Lommen, "New limits on gravitational radiation using pulsars," arXiv:astro-ph/0208572;  
 F. A. Jenet *et al.*, "Upper bounds on the low-frequency stochastic gravitational wave background from pulsar timing observations: Current limits and future prospects," Astrophys. J. **653**, 1571 (2006) [arXiv:astro-ph/0609013].
- [12] J. Polchinski, "Introduction to cosmic F- and D-strings,"

- arXiv:hep-th/0412244;  
 J. Polchinski, “Cosmic String Loops and Gravitational Radiation,” arXiv:0707.0888 [astro-ph].
- [13] J. Canny, “A computational approach to edge detection”, IEEE Trans. Pattern Analysis and Machine Intelligence **8**, 679 (1986).
- [14] P. D. Mauskopf *et al.* [Boomerang Collaboration], “Measurement of a Peak in the Cosmic Microwave Background Power Spectrum from the North American test flight of BOOMERANG,” Astrophys. J. **536**, L59 (2000) [arXiv:astro-ph/9911444].
- [15] C. L. Bennett *et al.*, “First Year Wilkinson Microwave Anisotropy Probe (WMAP) Observations: Preliminary Maps and Basic Results,” Astrophys. J. Suppl. **148**, 1 (2003) [arXiv:astro-ph/0302207].
- [16] A. Albrecht, D. Coulson, P. Ferreira and J. Magueijo, “Causality and the microwave background,” Phys. Rev. Lett. **76**, 1413 (1996) [arXiv:astro-ph/9505030].
- [17] L. Perivolaropoulos, “Spectral Analysis Of Microwave Background Perturbations Induced By Cosmic Strings,” Astrophys. J. **451**, 429 (1995) [arXiv:astro-ph/9402024].
- [18] J. Magueijo, A. Albrecht, D. Coulson and P. Ferreira, “Doppler peaks from active perturbations,” Phys. Rev. Lett. **76**, 2617 (1996) [arXiv:astro-ph/9511042].
- [19] U. L. Pen, U. Seljak and N. Turok, “Power spectra in global defect theories of cosmic structure formation,” Phys. Rev. Lett. **79**, 1611 (1997) [arXiv:astro-ph/9704165].
- [20] R. Jeannerot, “A Supersymmetric SO(10) Model with Inflation and Cosmic Strings,” Phys. Rev. D **53**, 5426 (1996) [arXiv:hep-ph/9509365];  
 R. Jeannerot, J. Rocher and M. Sakellariadou, “How generic is cosmic string formation in SUSY GUTs,” Phys. Rev. D **68**, 103514 (2003) [arXiv:hep-ph/0308134].
- [21] E. Witten, “Cosmic Superstrings,” Phys. Lett. B **153**, 243 (1985).
- [22] E. J. Copeland, R. C. Myers and J. Polchinski, “Cosmic F- and D-strings,” JHEP **0406**, 013 (2004) [arXiv:hep-th/0312067].
- [23] S. Sarangi and S. H. H. Tye, “Cosmic string production towards the end of brane inflation,” Phys. Lett. B **536**, 185 (2002) [arXiv:hep-th/0204074].
- [24] C. P. Burgess, “Inflatable string theory?,” Pramana **63**, 1269 (2004) [arXiv:hep-th/0408037];  
 J. M. Cline, “Inflation from string theory,” arXiv:hep-th/0501179;  
 A. Linde, “Inflation and string cosmology,” eConf **C040802**, L024 (2004) [arXiv:hep-th/0503195].
- [25] R. H. Brandenberger and C. Vafa, “Superstrings In The Early Universe,” Nucl. Phys. B **316**, 391 (1989).
- [26] A. Nayeri, R. H. Brandenberger and C. Vafa, “Producing a scale-invariant spectrum of perturbations in a Hagedorn phase of string cosmology,” Phys. Rev. Lett. **97**, 021302 (2006) [arXiv:hep-th/0511140];  
 R. H. Brandenberger, A. Nayeri, S. P. Patil and C. Vafa, “String gas cosmology and structure formation,” arXiv:hep-th/0608121.
- [27] U. Seljak and M. Zaldarriaga, “A Line of Sight Approach to Cosmic Microwave Background Anisotropies,” Astrophys. J. **469**, 437 (1996) [arXiv:astro-ph/9603033].
- [28] M. J. White, J. E. Carlstrom and M. Dragovan, “Interferometric Observation of Cosmic Microwave Background Anisotropies,” Astrophys. J. **514**, 12 (1999) [arXiv:astro-ph/9712195].
- [29] L. Perivolaropoulos, “COBE versus cosmic strings: An Analytical model,” Phys. Lett. B **298**, 305 (1993) [arXiv:hep-ph/9208247];  
 L. Perivolaropoulos, “Statistics of microwave fluctuations induced by topological defects,” Phys. Rev. D **48**, 1530 (1993) [arXiv:hep-ph/9212228].
- [30] G. F. Smoot *et al.*, “Structure in the COBE differential microwave radiometer first year maps,” Astrophys. J. **396**, L1 (1992).
- [31] A. A. Fraisse, C. Ringeval, D. N. Spergel and F. R. Bouchet, “Small-Angle CMB Temperature Anisotropies Induced by Cosmic Strings,” arXiv:0708.1162 [astro-ph].
- [32] The statistical properties of the long strings are much better established from numerical string evolution simulations than is the distribution of string loops. Different numerical codes all agree that the distribution of long strings scales. Even the number of long strings crossing each Hubble volume is known to within one order of magnitude. The distribution of cosmic string loops, however, much less well known. Even the form of the scaling distribution, not to mention the parameters of such a distribution, are unknown.
- [33] Initially [3], cosmic strings were studied as an alternative to inflation as a mechanism for structure formation.
- [34] Since the range of  $l$  values for which the CMBFAST program generates  $C_l$  values is limited to 3000, we are currently unable to explore angular scales relevant to upcoming experiments. We are at the moment completing an improved code which will allow us to obtain an improved angular resolution.
- [35] We thank Gil Holder for suggesting this method.